Inhibition of Copper Corrosion in Sulfuric Acid by *Mentha Pulegium L.*

S. Rached[1], K. Mzioud[1], A. Habsaoui[1], M. Galai[1*], K. Dahmani[2], M. Ouakki[2], S. EL Fartah[1], N. Dkhireche[1] and M. Ebn Touhami[1]

[1]*Advanced Material and Process Engineering, Faculty of Sciences, Ibn Tofaïl University, P.O. Box133, 14000, Kenitra, Morocco*
[2]*Laboratory of Organic, Inorganic Chemistry, Electrochemistry and Environment, Faculty of Sciences, Ibn Tofaïl University, P.O. Box 133, 14000, Kenitra, Morocco*
[*]Corresponding author: galaimouhsine@gmail. com

Received 21/03/2022; accepted 21/05/2022
https://doi.org/10.4152/pea.2024420205

Abstract
The application of inhibitors against metals and alloys corrosion in various aggressive environments is an excellent solution. The present study explored Cu corrosion inhibition in a 0.5 M H_2SO_4 solution by MP EO, from Western Morocco, using EIS and PDP analyses. GC coupled with MS revealed that MP EO is mainly composed of pulegone (23.38%), isomenthone (20.54%) and l-menthone (9.56%). MP inhibitory behavior was of mixed type. MO EO prevented Cu corrosion in H_2SO_4, with an IE(%) that increased with its Ct, at a maximum of 91.0%, with 1 g/L. The Cu surface was studied by SEM coupled with EDS.

Keywords: Cu, EDS, EIS, EO, GC, H_2SO_4, IE(%), MP, MS and SEM.

Introduction•

Metals are amongst the most widely used materials, particularly in mechanical engineering, transport industry, electronics and construction. However, metals and alloys usefulness is limited by the common problem of corrosion [1, 2]. Corrosion is defined as the deterioration of a metal, due to chemical attack or environmental reaction [3]. Cu is among the materials that are commonly used in heating and cooling systems, due to its excellent thermal conductivity and good mechanical workability [4, 5]. However, scale and corrosion products have a negative effect on heat transfer, and lead to a decrease in the equipment heating efficiency, which requires periodic descaling and cleaning with H_2SO_4 or HCl pickling solutions [6]. Recently, several studies have examined the possibility of using organic inhibitors mechanisms against metallic corrosion in different acidic media [7, 8, 9]. Considerable efforts have been made to find suitable compounds that inhibit metal corrosion in various aggressive environments [10]. Therefore, metals and alloys protection is of particular interest, and one approach is the use of corrosion inhibitors [11].
Many compounds that are green inhibitors have been investigated for their corrosion prevention potential [12]. All these studies state that organic compounds containing N, S and O in their structures have shown significant IE(%) [13]. These inhibitors retard metals corrosion by being adsorbed onto a metal surface. The adsorption process is influenced by factors such as the inhibitor molecular size and Ct, the substituents nature, T and nature of the test solution [14, 15]. Organic compounds and extracts from plants have been examined for their inhibitory properties, including caffeic acid [16], pennyroyal oil [17], caffeine [18],

•The abbreviations and kinetic parameters lists are in page 148.

thyme [19], jojoba oil [20], rosemary oil [21, 22] and eugenol [23]. Polymers, polymeric polyepoxides and epoxy resin [24-28], e.g., TGETBAE and HGTMDAE, are also used as metals corrosion inhibitors [29, 30]. EO are studied for their corrosion IE(%) that is linked to terpenoids, hydrocarbons and S compounds naturally present in different Ct [31, 32]. For the same plants, the EO nature and constituents amount differ according to their origin (climate, soil, altitude), which has a huge impact on their effectiveness. Within this framework, the present study aimed to determine the chromatographic analysis of MP EO, from the region of Zaër (Western Morocco), and to study its IE(%) for Cu corrosion in a 0.5 M H_2SO_4 medium, by varying two essential parameters: Ct and T.

Zaër region

Zaër region is of trapezoidal shape, located in the heart of Morocco, between the Atlas Mountains and the Atlantic Ocean, at 33° and 34° North latitude and 6° and 7° West longitude, and covers an area of approximately 3.860 Km^2. [33]. It is bordered to the north by the Rabat region, to the east by the Zemmour region, to the south-west by the Chaaouia region and to the south by the Beni Khiran domain. Cherrat, Bou Regreg and Grou rivers set their limits on nearly half of its length. The climate of this region is Mediterranean: mild and humid in winter, and hot and dry in summer; rainfall in the region far exceeds the national average [34].

Materials and methods

Plant material

The genus *Mentha* comprises 25 to 30 species that grow in temperate regions of Eurasia, Australia and South Africa, in the wetlands of plains and mountains up to 2200 meters above sea level [35]. MP, locally called *Fliou*, is also known as pouliot, royal pouliot, flea or chip hunt, and it belongs to the *Lamiaceae* family.

MP extraction

MP was collected from the region of Zaër, Morocco, in April. The extraction of its EO was carried out using a Clevenger apparatus: 230 g MP fresh leaves were introduced into a 2 L flask with distilled water (about 2/3 of the flask), and the mixture was boiled for 4 h. The EO extract (volatile part) was kept in the dark, at 4 ºC, for later use.

MP EO analyses by GC and MS

The MP EO volatile part analyses were carried out by GC and MS, at the Centre for Analysis, Expertise, Technology, Transfer and Incubator of the Ibn Tofail University, Kenitra. The analyses conditions were: ionization energy - 70 eV; T - 300 ºC; carrier gas - He; He flow rate - 1.70 mL; injection flow rate - 1 µl; injection volume - 1 mL; injection mode - Std Split/splitless; and total time - 40 min. GC was of the type 456 coupled to a MS type EVOQTQ. The column was Rxi - 5 sil MS (30 x 0.25mm ID X 0.25 µmdf) capillary type, the detector was FID and the software was MS DATA review, with a computerized database (NIST 2014).

WE preparation

The used Cu plate chemical composition (in %) was: 0.019 P, < 0.001 Fe, < 0.001 As, < 0.001 Mn, < 0.002 Sb, < 0.001 Al, 0.009 Sn, 0.003 Ni, 0.015 Pb, < 0.005 Ag, < 0.001 Bi, < 0.001 S, < 0.005 C and Cu (balance). The WE underwent a pre-treatment before each test, which consisted of polishing the electrode surface with different abrasive papers (800, 400, 1200 and 1500 grades), rinsing with distilled water, degreasing in acetone and drying.

Corrosive solution preparation

The corrosive solution was a 0.5 M H_2SO_4 aqueous solution, and its pH and T were maintained at 2 and 25 °C, respectively. Solutions of 0.5 M H_2SO_4 with MP EO were freshly prepared before each experiment.

Electrochemical measurements

Electrochemical measurements were performed using a PGZ100 potentiostat/galvanostat controlled by Volta Master 4 analysis software, in a H_2SO_4 0.5 M aqueous solution. The corrosion cell used was equipped with three electrodes: SC electrode ($Hg/HgCl_2$ in saturated KCl) and Pt wire were used as RE (DHW type) and CE, respectively. All E values given in this work refer to this RE by using a Cu plate as WE (with an exposed surface area of 1 cm^2). The experiments were carried out after 30 min immersion of Cu in a 0.5 M H_2SO_4 solution, without and with MP, at different Ct. The PDP curves were obtained by sweeping the WE E from -1200 to 600 mV, at a SR of 1 mV/s. All electrochemical experiments were performed at a T of 298 K. The Ct range used for MP was from 0.5 to 2 g/L. To evaluate the kinetic corrosion parameters, Stern-Geary equation was used. For this purpose, overall i values were taken as the sum of two contributions, i_a and i_c, respectively. For the E range not too far from OCP, both processes followed Tafel's law [36]. Thus, it can be derived from equation (1) that:

$$i = i_a + i_c = i_{corr}\{\exp [b_a \times (E - E_{corr})] - \exp [b_c \times (E - E_{corr})]\} \quad (1)$$

where i_{corr} is in A cm^{-2}, and β_a and β_c are in V/dec, at the usual logarithmic scale given by equation (2):

$$\beta = \ln 10/b = 2.303/b \quad (2)$$

The corrosion parameters were then evaluated by the NLLS method, applying equation (1), using the Origin software.

The corrosion IE(%) was evaluated from i_{corr} values using equation (3):

$$\eta_{pp} = i^0_{corr} - i_{corr} / i^0_{corr} \times 100 \quad (3)$$

where i^0_{corr} is i_{corr} value without MP. EIS diagrams were produced under the Nyquist plot. The results were then analyzed in terms of equivalent electrical circuit, using Bouckamp's program [37]. IE(%) was also calculated using the following equation (4):

$$\eta_{EIS} = R_{ct} - R^0_{ct} / R_{ct} \times 100 \quad (4)$$

where R^0_{ct} is R_{ct} value without MP.

Surface morphology analysis

To confirm the formation of a layer on the Cu surface immersed in a 0.5 M H_2SO_4 solution, for 16 h, with and without MP EO, SEM analysis coupled with EDX microanalysis were carried out at CNRST, Rabat, Morocco.

Results and discussion

EO yield

The extraction with Clevenger aparatus allowed to obtain two fractions: the EO, which is the volatile fraction, and the hydrolate, with a yield of 1.43% from 230 g MP fresh leaves. This content was approximately equal to that obtained by Derwich et al. (1.66%) [38].

Product analysis by GC/MS coupling

Through GC/MS analysis, it was possible to identify a total of 31 compounds for MP (listed in Table 1).

Table 1: MP EO composition.

N	Retention time (min)	Percentage (%)	Compound name
1	8.060	0.61	E-3-Hexenol
2	12.992	0.29	3-Methylcyclohexanone
3	13.787	0.11	(-)-β-Pinene
4	14.193	0.14	3-Octenol
5	14.582	0.44	Octan-3-ol
6	15.332	3.98	(+)-Limonene
7	15.364	0.45	Eucalyptol
8	18.114	20.54	Isomenthone
9	18.178	9.56	l-Menthone
10	18.565	5.51	Isopulegone
11	18.826	2.24	Menthol
12	18.983	1.9	3-hydroxy-4,4-dimethyldihydrofuran-2-one
13	19.035	0.66	(E)-2, 2, 5,5-tetramethyl-3-hexene
14	19.378	23.38	Pulegone
15	19.431	2.12	1-Dodecyne
16	19.466	3.08	(4Z)-2-isopropylhexa-1,4-diene
17	19.545	3.85	Cyclohexanone, 2-isopropylideno-5-methyl
18	19.619	1.37	(1R)-1-methoxymyodesertan
19	19.676	3.75	(Z)-6-methyl-5-methylene-2-heptene
20	19.704	2.59	Spiro[2.5]octane
21	19.766	3.01	2-Cyclohexyloxirane
22	20.146	0.14	Carbonic acid, (1R)-(-)-menthyldecyl ester
23	20.163	0.15	(S)-(+)-cis-Isopiperitenone
24	20.280	0.88	(7-Hydroxy-3,3-dimethyl-4-oxo-7-vinylbicyclo[3.2.0] hept-1-yl)acetaldehyde
25	20.325	0.80	Dihydroedulan
26	20.449	1.32	(-)-Neomenthylacetate
27	20.474	1.02	2-Isopropyl-3-methylcyclohexyl acetate
28	20.501	1.59	l-Menthol acetate
29	20.919	3.16	Piperitenone
30	22.334	1.19	Humulene
31	24.506	0.17	β-Acoradienol

MP EO extracted using Clevenger apparatus has pulegone as its main constituent, with a content of 23.38%, and also: (-)-beta-pinene (0.11%), 3-octenol (0.14%), octan-3-ol (0.44%), (+)-limonene (3.98%), eucalyptol (0.45%), isomenthone (20. 54%), l-menthone (9.56%), isopulegone (5.51%), menthol (2.24%), piperitenone (3.16%), l-menthol acetate (1.59%) and humulene (1.19%).

These compounds are considered to be good corrosion inhibitors, due to the presence of pulegone, as found in other work [39]. These results are compatible with most of the work already carried out in Morocco, which confirms that Moroccan MP EO is rich in pulegone [40]. The same is true for MP collected throughout the world, which shows that it belongs to the pulegonechemo type [41]. Several works have studied MP EO inhibition mechanism [42] but, to our knowledge, not against Cu corrosion in H_2SO_4.

PDP

Ct effect

Fig. 1 shows a set of polarization curves for the Cu electrode immersed in a 0.5 M H_2SO_4 solution without and with MP EO, at different Ct. Each polarization curve is

formed of two half curves, one representing anodic (Cu dissolution) and another cathodic domains (O reduction). The involved redox reactions are:

- Reduction reaction: $O_2 + 4\,H^+ + 4e^- \longrightarrow 2H_2O$
- Oxidation reaction: $Cu \longrightarrow Cu^{2+} + 2e$

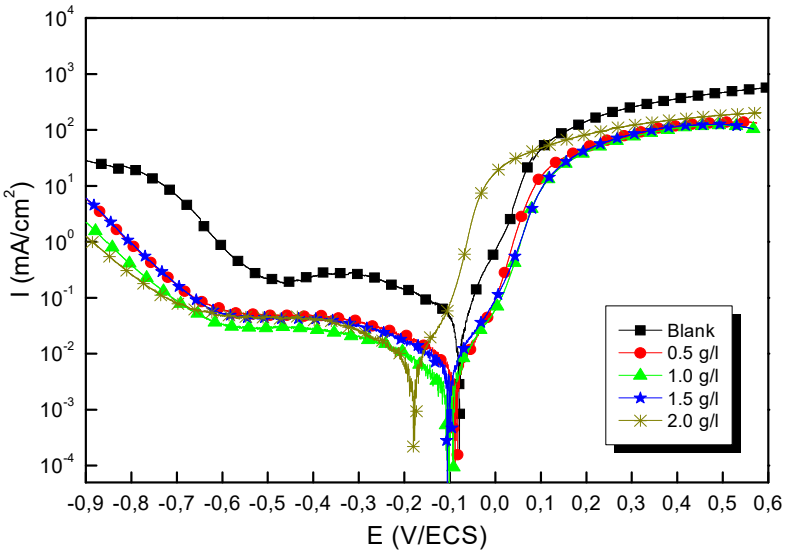

Figure 1: Polarization curves of Cu in 0.5 M H_2SO_4 solutions without and with MP EO.

Various studies have confirmed that, although MP EO has shown high IE(%) against metals corrosion, it is dependent on the extract Ct [43, 44]. For this study, by comparing the polarization curves, without and with MP EO, higher inhibitor Ct shifted E value in the negative direction, and caused a slight decrease in i_a and i_c densities. However, MP EO corrosion IE(%)was significant at a Ct of 1.0 g/ L, reaching the maximum value of 91.0%. Table 2 shows some examples in the literature of MP as a green corrosion inhibitor:

Table 2: Examples of MP used a corrosion inhibitor.

EO inhibitor	Medium	Type of metal	Maximum IE(%)	Ref
MP	1 M HCl	MS	90% at 1 g/L	[45]
	0.5 M H_2SO_4	MS	89.7% at 4g/ L	[46]
	2 M H_3PO_4	Aluminum	79% at 1800 ppm	[47]
	0.1 M Na_2CO_3	Aluminum	94.16% at 800 ppm	[48]
	0.5 M $H_2C_2O_4$	Tinplate	80% at 4 g/ L^{-1}	[49]

Kinetic parameters such as E_{corr}, i_{corr}, β_c, β_a and IE(%) are listed in Table 3.
In the literature, it has been reported that, if the displacement in E_{corr} is > 85 mV, the inhibitor can be considered cathodic or anodic, and if it is < 85 mV, it can be considered of the mixed type [50].
In our study, according to Table 3, we note that MP EO addition reduced i_{corr} from 29 to 2.4 µA/cm^{-2}. Thus, Cu resisted corrosion in the inhibitor presence. This may be due to MP EO adsorption onto the metal/acid interface. Nevertheless, the decrease in MP EO i_{corr}, compared to the blank 0.5 M H_2SO_4, for the anodic and

cathodic sites, may indicate a mixed type of corrosion inhibition. Moreover, the displacement of E_{corr}< 85 mV confirms the behavior of a mixed type inhibitor.

Table 3: Electrochemical parameters of the stationary polarization curve of Cu in a H_2SO_4 0.5 M medium.

Inhibitor	Ct g/L	E_{corr} (mV/ECS)	i_{corr} (µA/cm^{-2})	Tafel slopes (mV/dec^{-1})		IE(%)
				$-\beta_c$	β_a	
Blank	--	-79	29.0	204	59	-
MP	0.5	-80	5.0	189	56	82.7
	1.0	-86	2.6	183	52	91.0
	1.5	-89	3.7	185	53	87.2
	2.0	-169	4.3	187	54	85. 2

EIS

In order to better understand the phenomenon occurred on the metal/solution interface, we have drawn the impedance diagram shown in Fig. 2.

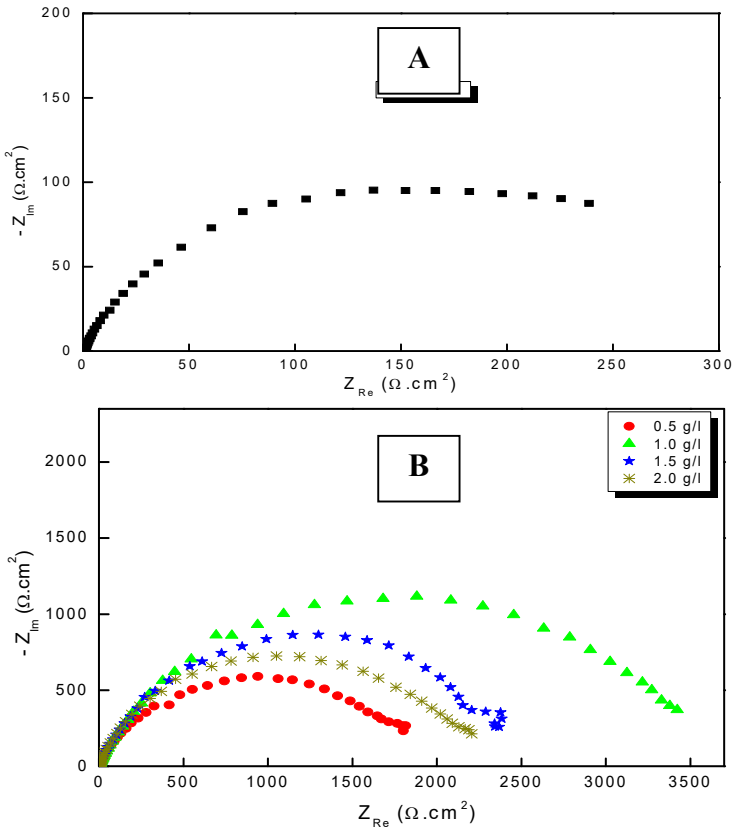

Figure 2: Nyquist plots for Cu in a 0.5 M H_2SO_4 solution: **(A)** without; and **(B)** with MP EO various Ct, at 298 K.

Through comparison of the uninhibited 0.5 M H_2SO_4 solution with the inhibited one, we notice that the display of the Cu impedance in the medium with MP EO changed considerably in shape and size (Fig. 2). The impedance data are simulated using the equivalent circuit illustrated in Fig. 4, for the electrode immersion in an H_2SO_4 solution containing MP EO, during only 60 min. The inhibitor caused

changes in impedance behavior. The increase in R_{ct} values was due to the development of a protective film at the metal-solution interface [51]. R_p diameter obviously increased, from 350/Ωcm^2, without MP EO, to over 3636 Ω/cm^2, with it (Table 4).

Table 4: Electrochemical parameters of the Cu electrochemical impedance curve.

Inhibitor	Ct g/L	R_s Ω/cm²	Q_f µF/cm²	n_f	R_f Ω/cm²	Q_{ct} µF/cm²	n_{ct}	R_{ct} Ω/cm²	R_p Ω/cm²	IE%
Blank	--	0.7±0.2	-	-	-	475±9.1	0.72±0.007	350±5.1	350	-
Inhibitor	0.5	2.3±0.9	35.9±4.8	0.903±0.007	94±7.1	150±4.4	0.569±0.008	1892±7.1	1986.0	82.4
	1.0	2.3±1.0	5.7±1.8	0.997±0.007	12.8±1.6	81.6±2.1	0.673±0.008	3624±14.2	3636.8	90.4
	1.5	1.8±1.0	9.9±1.7	0.998±0.007	18.7±1.4	96.4±3.8	0.673±0.008	2526±73.8	2544.7	86.2
	2.0	1.8±1.0	17.4±1.9	0.952±0.007	38.2±5.4	106.2±5.6	0.669±0.008	2264±12.5	2302.2	84.8

From the shape of the capacitive loops, we see that the corrosion process was controlled by a diffusion mechanism. This was confirmed by [52, 53]. The diameter of these capacitive loops increased progressively with higher MP EO Ct, which indicates a strengthening of the inhibitory film. The electrochemical parameters of these diagrams are shown in Table 4.
In Fig. 3, the condenser was replaced by a CPE, which indicated the presence of a dissimilar frequency response. CPE impedance is defined as follows [54]:

$$Z_{CPE}^{(\omega)} = Q^{-1}(j\omega)^{-n}$$

where Q is a constant in Ω/cm^2 in s^n, ω is the angular frequency in rad/s and n is CPE exponent, with -1< n< 1.
CPE can represent an inductance, a Warburg impedance, a pure capacitance, or a resistance, with n = - 1, 0.5, 0 and 1, respectively. The smaller the n value, the higher the surface roughness [55].

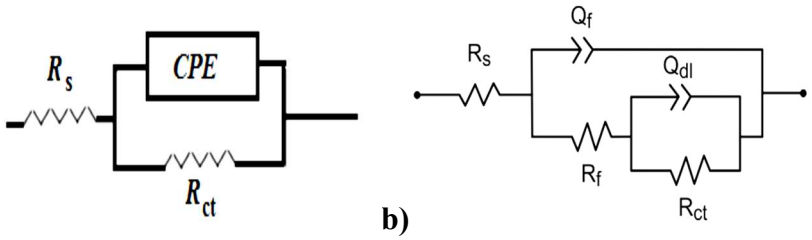

Figure 3: Equivalent circuits for Cu EIS used to model Cu/solution interface without **(a)** and **(b)** with MP EO.

T effect and thermodynamic parameters
The T of the corrosive environment is one of the factors that can modify the behavior of materials in a given corrosive environment, as well as the IE(%) of a compound. In general, as T increases, changes in the inhibitor action occur.
Due to the importance of this factor, trace tests of the polarization curves for the 0.5 M H_2SO_4/Cu interface with and without MP EO, at different T, were performed. They are shown in Figs. 4 and 5.

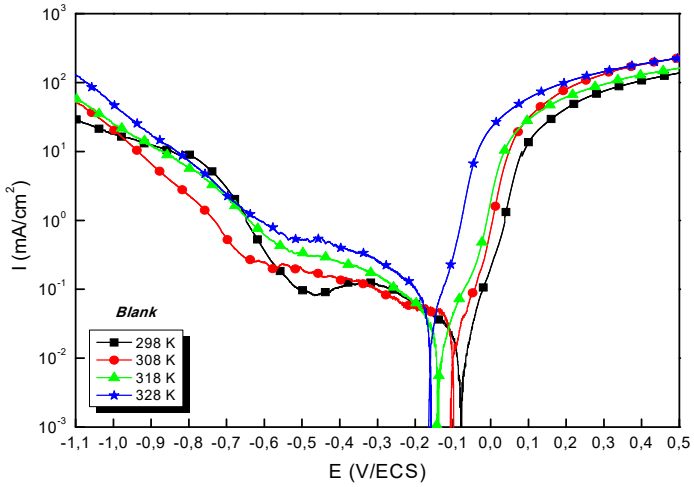

Figure 4: PDP curve for Cu in 0.5 M H_2SO_4 without MP EO, at different T.

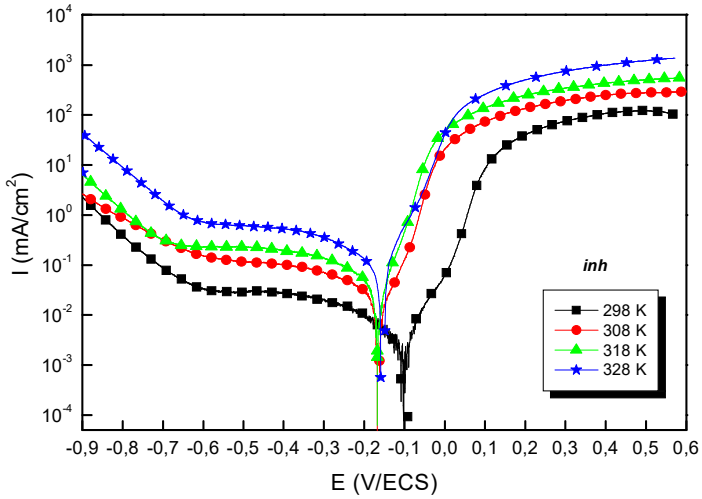

Figure 5: PDP curve for Cu in 0.5M H_2SO_4 with MP EO, at different T.

The electrochemical parameters from these diagrams are shown in Table 5.

Table 5: Electrochemical parameters from the stationary polarization curves of Cu without and with MP, at different T.

Compound	T (K)	$-E_{corr}$ (mV/ECS)	i_{corr} (µA/cm²)	$-\beta_c$ (mV)	β_a (mV)	IE(%)
Blank	298	79	29.0	204	59	-
	308	105	35.0	188	64	-
	318	142	56.0	164	77	-
	328	166	77.0	152	52	-
1.0 g/L MP	298	86	2.6	183	52	91.0
	308	164	3.8	171	56	89.1
	318	166	7.2	152	66	87.2
	328	159	11.8	143	70	84.6

Theoretically, higher T increase PDP curves i value and decrease IE(%) [56]. This is illustrated more clearly, in Table 4, by i_{corr} variation with T: i varied from 29.0 to 77.0 µA/cm^{-2}, at 298 and 328 K, respectively. CR dependence on T can be expressed by Arrhenius equation:

$$i_{corr} = (-E_a/RT) \quad (5)$$

where A is the frequency factor and R is universal gas constant (8.314 J/mol^{-1}/K^{-1}). The Arrhenius plot that obtained Ln i_{corr} as a function of 1000/T is shown in Fig. 6, and is compared with that of Cu in a 0.5 M H_2SO_4 solution without EO. The experimental curve obtained for MP EO corresponded approximately to a straight line, and anodic E value was determined from the slope of this line. In addition, other kinetic parameters, such as ΔH_{ads} and ΔS_{ads}, were obtained from the following transition state equation:

$$Ln\left(\frac{I_{corr}}{T}\right) = \left(Ln\left(\frac{R}{Nh}\right) + \frac{\Delta Sa}{R}\right) - \frac{\Delta Ha}{RT}$$

where h is Plank's constant and N is Avogrado's number.

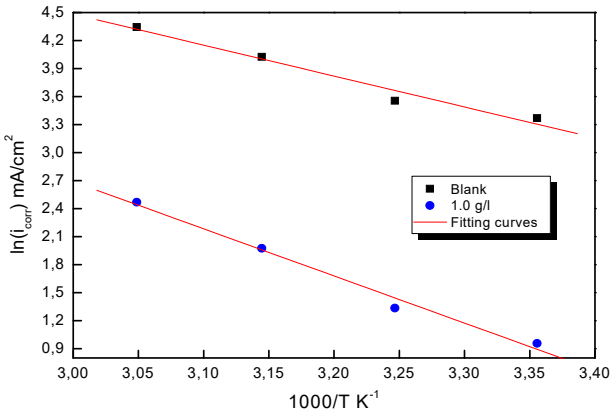

Figure 6: Arrhenius plots for Cu in 0.5 M H_2SO_4 without and with MP EO.

Ln (i_{corr}/T) variation as a function of 1000/T in 0.5 M H_2SO_4 gave a straight line, as shown in Fig. 7, with a slope of -ΔH_a/R. The intersection with the x-axis is Ln (R/Nh) + (ΔH_a/R).

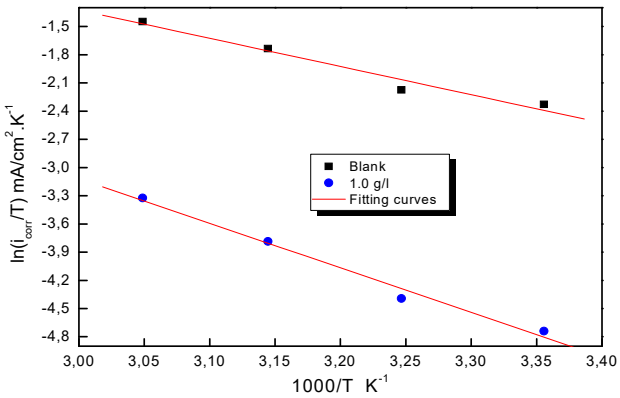

Figure 7: Arrhenius diagrams of Ln (i_{corr}/T) versus 1000/T for Cu in 0.5 M H_2SO_4 without and with MP EO.

Adjustment of the curve (Fig. 7) with a straight line gave a value of 41.9 kJ/mol^{-1} for the corrosion process E_a with MP EO. This value is much higher than that for

Cu without MP (27.50 kJ mol^{-1}), which explains why the variations in i_{corr} were more pronounced with the inhibitor (Table 6).

Table 6: Values of E_a, ΔH_a and ΔS_a kinetic parameters for Cu in 0.5 M H_2SO_4 without and with MP EO.

Compound	E_a (kJ/mol^{-1})	ΔH_a (kJ/mol^{-1})	ΔS_a (J/mol^{-1}/k^{-1})
Blank	27.50	25.00	-134.0
1.0 g/L MP	41.9	39.3	-105.3

The increase in anodic E_{corr}, in MP EO presence, associated with a decrease in IE(%), with higher T, is frequently understood as being due to the formation of an adsorption film of a physical nature, i.e. involving electrostatic interactions with the metal surface, according to Popova et al. [57]. The results of the present work suggested a predominant physisorption inhibition. However, ΔH_a positive signs reflect Cu dissolution process endothermic nature. Indeed, higher ΔH_a in MP EO presence corresponds to a decrease in the metal dissolution.

Surface analysis

To confirm the results obtained by electrochemical measurements, the surface morphology of Cu samples with and without MP EO, after 16 h of immersion, was studied by SEM (Fig. 8), and the chemical composition was obtained by EDX microanalysis (Fig 9).

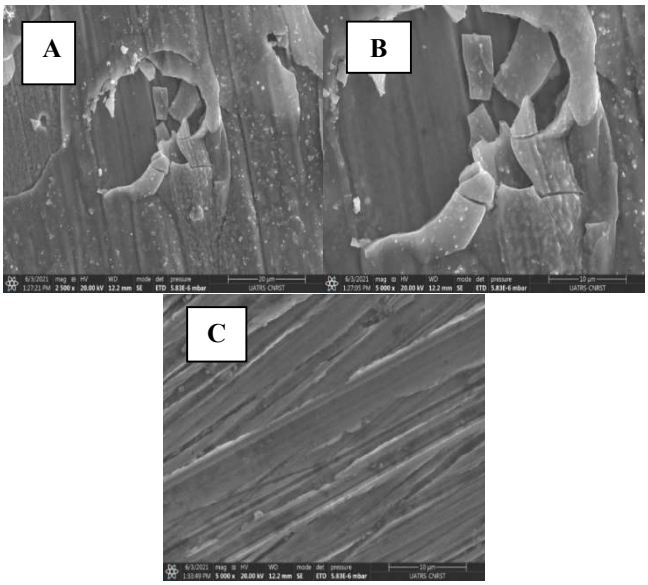

Figure 8: SEM images of the Cu surface immersed in 0.5 M H_2SO_4 solutions, for 16 h, at 298 K: **A** and **B-** without inhibitor; and **C** with inhibitor.

The results show that: the Cu coupon control sample (Fig. 8 A and B), immersed in 0.5 M H_2SO_4 without MP EO, was very damaged, since it had a very rough surface, with corrosion products and cracks, due to the attack by the aggressive solution, showing pronounced dissolution; MP EO addition caused a decrease in

Cu degree of corrosion, with cracks disappearance and a regular and smoother morphology (Fig. 8 C), which indicates the formation of a protective film on the metal surface; EDX microanalysis (Fig. 9) shows a decrease in O percentage, and the disappearance of S peak after MP EO addition. Since S and O corrode Cu, their decrease explains the metal surface regularity during the treatment with MP EO. This was due to the formation of a film on the Cu surface by the inhibitor molecules, which protected it from the corrosive attack; therefore, SEM images and EDX microanalysis results are consistent with those of PDP and EIS tests.

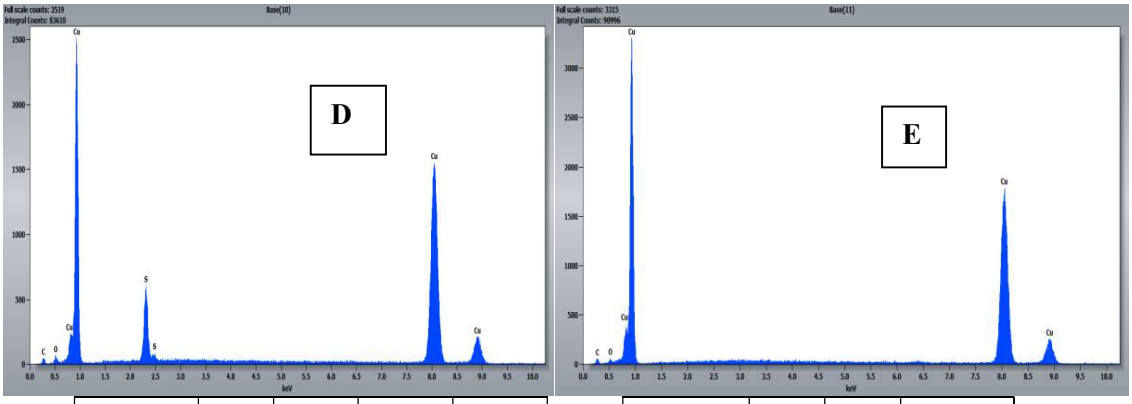

Element	C	O	S	Cu
Wt.%	4.55	2.00	9.39	84.07

Element	C	O	Cu
Wt.%	4.48	0.73	94.79

Figure 9: EDX spectra for the Cu surface in 0.5 M H_2SO_4 solutions, for 16 h, at 298 K: **D**- without inhibitor; and **E**- with inhibitor.

Conclusion

This work was part of a long and important line of research aimed at valorizing natural plant resources, in particular, the aromatic and medicinal plants of Morocco. In this context, we have chosen to study MP from the Zaër region, based on traditional uses by the Moroccan population. At the end of this study, we can deduce the following conclusions: GC/MS analyses of MP EO allowed to determine its chemical composition, and pulegone was determined as the major compound; MP EO acted as Cu corrosion inhibitor in 0.5 M H_2SO_4; MP EO IE(%) reached 91.0% at a Ct of 1.0 g/L; MP EO acted as a mixed inhibitor, and its IE(%) increased with higher T.

Conflict of interest

The authors declare that they have no known competing financial interests or personal relationships that could have appeared to influence the work reported in this paper.

Authors' contributions

S. Rached: wrote the paper. **K. Mzioud**: collected the data. **A. Habsaoui**: conceived and designed the analysis. **M. Galai**: conceived and designed the analysis. **K. Dahmani**: collected the data. **M. Ouakki**: performed the analysis. **S. EL Fartah**: collected the data. **N. Dkhireche**: wrote the paper. **M. Ebn Touhami**: inserted data or analysis tools.

Abbreviations

β_a: anodic Tafel slope constant
β_c: cathodic Tafel slope constant
Ct: concentration
CE: counter electrode
CPE: constant phase element
CR: corrosion rate
E: potential
E_{corr}: corrosion potential
EDS: energy dispersive X-ray
EIS: electrochemical impedance spectroscopy
EO: essential oil
GC: gas chromatography
$H_2C_2O_4$: oxalic acid
H_2SO_4: sulphuric acid
H_3PO_4: phosphoric acid
HCl: hydrochloric acid
HGTMDAE: hexaglycidyltrimethylenedianiline of ethylene
i: current density
i_a: anodic current
i_c: cathodic current
i_{corr}: corrosion current density
IE(%): inhibition efficiency
MP: Mentha pulegium
MS: mass spectrometry
Na_2CO_3: sodium carbonate
NLLS: non-linear least square
OCP: open-circuit potential
PDP: potentiodyamic polarization
R_{ct}: charge transfer resistance
Redox: reduction-oxidation reactions
RE: reference electrode
R_p: polarization resistance
SC: saturated calomel
SEM: scanning electron microscopy
SR: scan rate
T: temperature
TGETBAE: triglycidyl ether tribisphenol A of ethylene
WE: working electrode

Kinetic parameters abbreviations

ΔH_a: activation enthalpy
ΔS_a: activation entropy
ΔH_{ads}: enthalpy of adsorption
ΔS_{ads}: entropy of adsorption
E_a: activation energy

References

1. Mouhsine G, Mohamed R, Kacimi Y et al. Anti-corrosion properties of sometriphenylimidazole substituted compounds in corrosion inhibition of carbon steel in 1.0 M hydrochloric acid solution. Analyt Bioanalyt Electrochem. 2017;9:80-101. https://www.sid.ir/en/Journal/ViewPaper.aspx?ID=660703
2. Erramli H, Dagdag O, Safi Z et al. Trifunctional epoxy resin as anticorrosive material for carbon steel in 1 M HCl: Experimental and computational studies. Surf Interf. 2020;21:100707. https://doi.org/10.1016/j.surfin.2020.100707
3. Rbaa M, Galai M, Benhiba F et al. Synthesis and investigation of quinazoline derivatives based on 8-hydroxyquinoline as corrosion inhibitors for mild steel in acidic environment: experimental and theoretical studies. Ionics. 2019;(25)7:3473-3491. https://doi.org/10.1007/s11581-018-2817-7
4. Dkhireche N, Galai M, ElKacimi Y et al. New Quinoline Derivatives as Sulfuric Acid Inhibitors for Mild Steel. Analyt Bioanalyt Electrochem. 2018;10(1):111-135. https://www.sid.ir/FileServer/JE/55002820180108.pdf
5. Dhouibi I, Masmoudi F, Bouaziz M et al. A study of the anti-corrosive effects of essential oils of rosemary and myrtle for copper corrosion in chloride media. Arab J Chem. 2021;14(2):102961. https://doi.org/10.1016/j.arabjc.2020.102961
6. Galai M, El Faydy M, El Kacimi Yet al. Synthesis, characterization and anti-corrosion properties of novel quinolinol on C-steel in a molar hydrochloric acid solution. Port Electrochim Acta. 2017;(35)4:233-251. https://doi.org/10.4152/pea.201704233
7. Hsissou R, Benzidia B, Hajjaji N et al. Elaboration and electrochemical studies of the coating behavior of a new nano functional epoxy polymer on E24 steel in 3.5% NaCl. Port Electrochim Acta. 2018;36(4):259-270. https://doi.org/10.4152/pea.201804259
8. El Faydy M, Galai M, Touir R et al. Experimental and theoretical studies for steel XC38 corrosion inhibition in 1 M HCl by N-(8-hydroxyquinolin-5-yl)-methyl)-N-phenylacetamide. J Mater Environ Sci. 2016;7(4):1406-16. https://www.jmaterenvironsci.com/Document/vol7/vol7_N4/155-JMES-2265-El%20Faydy.pdf
9. Dahmani K, Galai M, Elhasnaoui A et al. Corrosion resistance of electrochemical copper coating realized in the presence of essential oils. Pharma Chem. 2015;7:566. http://derpharmachemica.com/archive.html
10. Essaadaoui Y, Galai M, Ouakki M et al. Study of the anticorrosive action of *Eucalyptus camaldulensis* extract in case of mild steel in 1.0 M HCL. J Chem Technol Metallur. 2019;(54)2:18-77. https://dl.uctm.edu/journal/node/j2019-2/24_18-77_p431-442
11. Verma CH, Quraishi M. Gum Arabic as an environmentally sustainable polymeric anticorrosive material: Recent progresses and future opportunities. Int J Bio Macromol. 2021;(184):118-134. https://doi.org/10.1016/j.ijbiomac.2021.06.050
12. Chaubey N, Qurashi A, Chauhan DS et al. Frontiers and advances in green and sustainable inhibitors for corrosion applications: A critical review. J Mol Liq. 2021;(321):114385. https://doi.org/10.1016/j.molliq.2020.114385
13. Mzioud K, Habsaoui A, Ouakki M et al. Inhibition of copper corrosion by the essential oil of *Allium sativum* in 0.5 M H_2SO_4 solutions. S N Appl Sci. 2020;(2)9:1-13. https://doi.org/10.1007/s42452-020-03393-8

14. Ajeigbe SO, Basar N, Hassan M et al. Optimization of corrosion inhibition of essential oils of *Alpinia galanga* on mild steel using response surface methodology. ARPN J Eng Appl Sci. 2017;12(9):2763-2771. https://www.researchgate.net/publication/317213370
15. Oguntade TI, Ita CS, Oyekunle D et al. Inhibition of mild steel corrosion using binary mixture of sesame and castor oil. Int J Phys. 2019;(1378)4:042009. https://iopscience.iop.org/article/10.1088/1742-6596/1378/4/042009/meta
16. Verma C, Ebenso EE, Quraishi MA. Ionic liquids as green and sustainable corrosion inhibitors for metals and alloys: an overview. J Mol Liq. 2017;233:403-414. https://doi.org/10.1016/j.molliq.2017.02.111
17. Khadraoui A, Khelifa A, Hadjmeliani M et al. Extraction, characterization and anti-corrosion activity of *Mentha pulegium* oil: weight loss, electrochemical, thermodynamic and surface studies. J Mol Liq. 2016;(216):24-731. https://doi.org/10.1016/j.molliq.2016.02.005
18. Kouakou V, Niamien P, Yapo AJ et al. Experimental and DFT studies on the behavior of caffeine as effective corrosion inhibitor of copper in 1 M HNO3. Orbital: Electronic J Chem. 2016;8(2):66-79. http://dx.doi.org/10.17807/orbital.v8i2.804
19. Verma C, Ebenso EE, Bahadur I et al. An overview on plant extracts as environmental sustainable and green corrosion inhibitors for metals and alloys in aggressive corrosive media. J Mol Liq. 2018;266:577-590. https://doi.org/10.1016/j.molliq.2018.06.110
20. AL-Lamei AJ, Muftin NK, Hussein FM et al. Organic Compounds as Corrosion Inhibitors from Natural Products. Int J Adv Res Phys Sci. 2020;7: 25-35. https://www.arcjournals.org/pdfs/ijarps/v7-i4/5.pdf
21. Jyothi S, Rao YS, Ratnakumar PS. Natural products as corrosion inhibitors in various corrosive media: a review. Rasayan J Chem. 2019;12(2):537-44. http://dx.doi.org/10.31788/RJC.2019.1225000
22. Bendahou M, Benabdellah M, Hammouti B. A study of rosemary oil as a green corrosion inhibitor for steel in 2 M H_3PO_4. Pigm Resin Technol. 2006. https://doi.org/10.1108/03699420610652386
23. Samontha A, Lugsanangarm K. Corrosion inhibition and adsorption mechanism of eugenol on copper in HCl medium. Prot Met Phys Chem Surfaces. 2019; 55(1):187-194. https://doi.org/10.1134/S2070205119010192
24. Hsissou R, Benhiba F, Echihi S et al. Performance of curing epoxy resin as potential anticorrosive coating for carbon steel in 3.5% NaCl medium: Combining experimental and computational approaches. Chem Phys Lett. 2021;783:139081. https://doi.org/10.1016/j.cplett.2021.139081
25. Hsissou R, Benhiba F, Echihi S et al. New epoxy composite polymers as potential anticorrosive coatings for carbon steel in 3.5% NaCl solution: Experimental and computational approaches. Chem Data Coll. 2021;31:100619. https://doi.org/10.1016/j.cdc.2020.100619
26. Hsissou R, Abbout S, Benhiba F et al. Insight into the corrosion inhibition of novel macromolecular epoxy resin as highly efficient inhibitor for carbon steel in acidic mediums: Synthesis, characterization, electrochemical techniques, AFM/UV–Visible and computational investigations. J Mol Liq. 2021;337:116492.https://doi.org/10.1016/j.molliq.2021.116492

27. Hsissou R. Review on epoxy polymers and its composites as potential anticorrosive coatings for carbon steel in 3.5% NaCl solution: Computational approaches. J Mol Liq. 2021;336:116307. https://doi.org/10.1016/j.molliq.2021.116307
28. Hsissou R, Abbout S, Safi Z et al. Synthesis and anticorrosive properties of epoxy polymer for CS in [1 M] HCl solution: Electrochemical, AFM, DFT and MD simulations. Constr Build Mat. 2021;270:121454. https://doi.org/10.1016/j.conbuildmat.2020.121454
29. Hsissou R, Bekhta A, Elharfi A et al. Theoretical and electrochemical studies of the coating behavior of a new epoxy polymer: hexaglycidylethylene of methylene dianiline (HGEMDA) on E24 steel in 3.5% NaCl. Port Electrochim Acta. 2018;36(2):101-117. https://doi.org/10.4152/pea.201802101
30. Hsissou R, Benzidia B, Hajjaji N et al. Elaboration, electrochemical investigation and morphological study of the coating behavior of new polymeric polyepoxide architecture: crosslinked and hybrid decaglycidyl of phosphorus pentamethylenedianiline on E24 carbon steel in 3.5% NaCl. Port Electrochim Acta. 2019;37(3):179-191. https://doi.org/10.4152/pea.201903179
31. Lazrak J, El Assiri El H, Arrousse N et al. *Origanum compactum* essential oil as a green inhibitor for mild steel in 1 M hydrochloric acid solution: Experimental and Monte Carlo simulation studies. Mat Today: Proceed. 2021;(45):7486-7493. https://doi.org/10.1016/j.matpr.2021.02.233
32. Dahmani K, Galai M, Ouakki M et al. Corrosion inhibition of copper in sulfuric acid via environmentally friendly inhibitor (*Myrtus communis*): Combining experimental and theoretical methods. J Mol Liq. 2022;347:117982. https://doi.org/10.1016/j.molliq.2021.117982
33. Lahsissene H, Kahouadji A, Hseini S et al. Catalog of medicinal plants used in the Zaër region (Western Morocco). Lejeunia. 2009;186:25. https://www.cabdirect.org/cabdirect/abstract/20103040931
34. Bouchaib S, Messaad SA, Khallaf M et al. Physico-chemical and bacteriological characterization of liquid effluents of two large hospitals in the Rabat-Salé-ZemmourZaer region. Int J Innov Appl Stud. 2014;9(4):1949-1955. https://www.researchgate.net/publication/270567378
35. Boukhebti H, Chaker AN, Belhadj H et al. Chemical composition and antibacterial activity of *Mentha pulegium L.* and *Menthaspicata L.* essential oils. Der Pharmacia Lett. 2011;3(4):267-275. http://scholarsresearchlibrary.com/archive.html
36. Stern M, Geary AL. Electrochemical polarization: I. a theoretical analysis of the shape of polarization curves. Journal of the electrochemical society. 1957;(104)1:56. https://iopscience.iop.org/article/10.1149/1.2428496/meta
37. Aal MA, Radwan S, El-Saied A. Phenothiazines as corrosion inhibitors for zinc in NH_4Cl solution. Brit Corros J. 1983;18(2):102-106. https://doi.org/10.1179/000705983798273903
38. Derwich E, Benziane Z, Taouil R et al. Comparative essential oil composition of leaves of *Mentharotun difolia* and *Mentha pulegium* as traditional herbal medicine in Morocco. Am Euras J Sust Agric. 2010;(4)1:47-54. https://www.researchgate.net/publication/267030913
39. Fouda A, S El-Abbasy HM, Badr AH. Natural Fenugreek Seeds as an Eco-Friendly Corrosion Inhibitor for Steel in Aqueous Solutions. Mat Sci. 2015; 33559-33562. https://www.researchgate.net/publication/282973088

40. Amalich S, Zerkani H, Cherrat A et al. Study on *Mentha Pulegium* L. from M'rirt (Morocco): Antibacterial and antifungal activities of a pulegone-rich essential oil. J Chem Pharm Res. 2016;(8):363-70. https://www.researchgate.net/publication/331716161
41. Chebli B, Achouri M, Idrissi LM et al. Chemical composition and antifungal activity of essential oils of seven Moroccan *Labiatae* against *Botrytis cinerea* Pers: Fr. J Ethnopharmacol. 2003;(89)1:165-169. https://doi.org/10.1016/S0378-8741(03)00275-7
42. Khadraoui A, Khelifa A, Hadjmeliani M et al. Extraction, characterization and anti-corrosion activity of oil: weight loss, electrochemical, thermodynamic and surface studies. J Mol Liq. 2016;216:724-731. https://doi.org/10.1016/j.molliq.2016.02.005
43. Benmessaoud LD, Zertoubi M, Irhzo A et al. Review: Plant oils and extracts as corrosion inhibitors for various metals and alloys in hydrochloric acid medium. J Mater Environ Sci. 2013;(6)4:855-866 2013. https://www.researchgate.net/publication/261709484
44. Chraibi M, Benbrahim KF, Elmsellem H et al. Antibacterial activity and corrosion inhibition of mild steel in 1.0 M hydrochloric acid solution by *M. piperita* and *M. pulegium* essential oils. J Mat Environml Sci. 2017;8(3):972-981. http://www.jmaterenvironsci.com
45. Galai M, Rbaa M, Ouakki M et al. Chemically functionalized of 8-hydroxyquinoline derivatives as efficient corrosion inhibition for steel in 1.0 M HCl solution: Experimental and theoretical studies. Surf Interfaces. 2020;21. https://doi.org/10.1016/j.surfin.2020.100695
46. Alaoui K et al. Poly (1-phenylethene): as a novel corrosion inhibitor for carbon steel/hydrochloric acid interface. 2016:830-847. https://www.sid.ir/en/Journal/ViewPaper.aspx?ID=660730
47. Uwineza MS, Essahli M, Lamiri A. Corrosion inhibition of aluminium in 2 M phosphoric acid using the essential oil of *Mentha pulegium* leaves. Port Electrochim Acta. 2016;34(1):53-62. https://doi.org/10.4152/pea.201601053
48. Imane H, Mohamed E, Abdeslam L. Inhibition of Aluminum Corrosion in 0.1 M Na_2CO_3 by *Mentha Pulegium*. Port Electrochim Acta. 2019;37(6):335-344. https://doi.org/10.4152/pea.201906335
49. Boumezzourh A, Ouknin M, Chibane E et al. Inhibition of tinplate corrosion in 0.5 M $H_2C_2O_4$ medium by *Mentha pulegium* essential oil. Int J Corros Scale Inhib. 2020;9(1):152-170.https://dx.doi.org/10.17675/2305-6894-2020-9-1-9
50. Cruz-Borbolla J, Garcia-Ochoa E, Narayanan J et al. Electrochemical and theoretical studies of the interactions of a pyridyl-based corrosion inhibitor with iron clusters (Fe15, Fe30, Fe45, and Fe60). J Mol Model. 2017;23(12): 1-15. https://doi.org/10.1007/s00894-017-3510-x
51. Elmsellem H, Basbas N, Chetouani A et al. Quantum chemical studies and corrosion inhibitive properties of mild steel by some pyridine derivatives in 1 N HCl solution. Port Electrochim Acta. 2014;(32)2:77-108. https://doi.org/10.4152/pea.201402077
52. Errahmany N, Rbaa M, Abousalem AS et al. Experimental, DFT calculations and MC simulations concept of novel quinazolinone derivatives as corrosion inhibitor for mild steel in 1.0 M HCl medium. J Mol Liq 2020;312. https://doi.org/10.1016/j.molliq.2020.113413
53. Shivakumar SS, Mohana KN. Studies on the inhibitive performance of *Cinnamomum zeylanicum* extracts on the corrosion of mild steel in hydrochloric acid and sulphuric acid media. J Mat Environ Sci. 2013;4(3):448-459. https://www.researchgate.net/publication/287708465

54. Galai M, Ouassir J, EbnTouhami M et al. α-Brass and (α+ β) Brass Degradation Processes in Azrou Soil Medium Used in Plumbing Devices. J Bio- Tribo-Corros. 2017;3:30. https://doi.org/10.1007/s40735-017-0087-y
55. Alaoui K, El Kacimi Y, Galai M et al. Anti-corrosive properties of polyvinyl-alcohol for carbon steel in hydrochloric acid media: electrochemical and thermodynamic investigation. J Mater Environ Sci. 2016;(7)7:2389-2403. https://www.researchgate.net/publication/303299068
56. Ouakki M, Galai M, Rbaa M et al. Quantum chemical and experimental evaluation of the inhibitory action of two imidazole derivatives on mild steel corrosion in sulphuric acid medium. Heliyon. 2019;5:e02759. https://doi.org/10.1016/j.heliyon.2019.e02759
57. Popova A, Sokolova E, Raicheva S et al. AC and DC study of the temperature effect on mild steel corrosion in acid media in the presence of benzimidazole derivatives. Corros Sci. 2003;45(1):33-58. https://doi.org/10.1016/S0010-938X(02)00072-0